

# Optical and structural properties of polycrystalline CVD diamond films grown on fused silica optical fibres pre-treated by high-power sonication seeding

R. Bogdanowicz · M. Śmietana · M. Gnyba ·  
Ł. Gołunski · J. Ryl · M. Gardas

Received: 20 January 2014 / Accepted: 25 February 2014 / Published online: 15 March 2014  
© The Author(s) 2014. This article is published with open access at Springerlink.com

**Abstract** In this paper, the growth of polycrystalline chemical vapour deposition (CVD) diamond thin films on fused silica optical fibres has been investigated. The research results show that the effective substrate seeding process can lower defect nucleation, and it simultaneously increases surface encapsulation. However, the growth process on glass requires high seeding density. The effects of suspension type and ultrasonic power were the specific objects of investigation. In order to increase the diamond density, glass substrates were seeded using a high-power sonication process. The highest applied power of sonotrode reached 72 W during the performed experiments. The two, most common diamond seeding suspensions were used, i.e. detonation nanodiamond dispersed in (a) dimethyl sulfoxide and (b) deionised water. The CVD diamond nucleation and growth processes were performed using microwave plasma assisted chemical vapour deposition system. Next, the seeding efficiency was determined and compared using the numerical analysis of scanning electron microscopy images. The molecular composition of nucleated diamond

was examined with micro-Raman spectroscopy. The  $sp^3/sp^2$  band ratio was calculated using Raman spectra deconvolution method. Thickness, roughness, and optical properties of the nanodiamond films in UV–vis wavelength range were investigated by means of spectroscopic ellipsometry. It has been demonstrated that the high-power sonication process can improve the seeding efficiency on glass substrates. However, it can also cause significant erosion defects at the fibre surface. We believe that the proposed growth method can be effectively applied to manufacture the novel optical fibre sensors. Due to high chemical and mechanical resistance of CVD diamond films, deposition of such films on the sensors is highly desirable. This method enables omitting the deposition of an additional adhesion interlayer at the glass–nanocrystalline interface, and thus potentially increases transmittance of the optical system.

## 1 Introduction

Due to a number of advantages, such as light weight, small size, large bandwidth, and resistance to electromagnetic field, optical fibres have found applications not only in telecommunication, but also in sensing [1]. The optical fibre sensors are used to measure with a great accuracy pressure [2], mechanical deformation [3], temperature [4] as well as concentration of gases [5], and composition of liquids [6]. However, under harsh environmental conditions, the use of silica glass fibres is difficult due to their poor resistance to mechanical impact and aggressive chemical influences. It has been reported that the application of diamond coating on fused silica optical fibres increases the Young modulus [7] and slightly decreases stress voids on the coating surface, especially at the

---

R. Bogdanowicz (✉) · M. Gnyba · Ł. Gołunski · M. Gardas  
Department of Metrology and Optoelectronics, Faculty of  
Electronics, Telecommunications and Informatics, Gdansk  
University of Technology, 11/12 G. Narutowicza Str,  
80-233 Gdańsk, Poland  
e-mail: rbogdan@eti.pg.gda.pl

M. Śmietana  
Institute of Microelectronics and Optoelectronics, Warsaw  
University of Technology, Koszykowa 75, 00-662 Warsaw,  
Poland

J. Ryl  
Department of Electrochemistry, Corrosion and Material  
Engineering, Gdansk University of Technology,  
11/12 Narutowicza Str., 80–233 Gdańsk, Poland

beginning of film growth [8]. Moreover, diamond films have one more great advantage, namely, they are optically transparent in a wide spectral range. Optical absorption in the range between 300 and 1,100 nm highly depends on defect density, chemical composition, doping level, the film thickness, and the grain size [9]. Developing diamond films that display good adhesion to the optical fibre's surface will allow for designing a new type of optical sensors. The novel sensors will offer improved mechanical and chemical durability as well as increased sensitivity [10]. Deposition of uniform thin films, entirely coating the glass fibres, is one of the biggest challenges. Moreover, the cylindrical shape of fibres, which is not compatible with deposition systems designed for flat substrates, and poor adhesion of the carbon-based films to fused silica [11] make the deposition of high-quality diamond films on optical fibres difficult. May et al. [12] demonstrated that it is possible to deposit highly resistive diamond on optical fibres. Also, the attempts to coat fused silica fibres with diamond or other carbon-based material have been reported. These materials have improved mechanical properties [8, 12, 13] and the fibre's resistance to high temperatures [7]. Moreover, Alberto et al. [13] have demonstrated that the diamond-coated fibre Bragg gratings (FBGs) exhibit improved stability to thermal annealing and mechanical deformation, and thus can be used as sensing element in harsh environment.

In the case of DLC layers, it is well-known that the substrate influences the film's optical properties [14]. In addition, the possibility of coating fused silica glass fibres with DLC was investigated [14]. When applied in sensing, the DLC-coated device shows fast response to variations in the concentration of chemical solution, e.g. ethylene glycol, human urine or sucrose [10].

Spectroscopic ellipsometry measurements have shown that the deposited carbon layers can be modelled using a multilayer corresponding to microstructural character of the layers [15–18]. Gupta et al. reported on the optical properties of thin diamond layers [19–21] and other types of carbon layers [22, 23]. The work of Hu et al. demonstrated that the optical properties of nanocrystalline (NCD) layers strongly depend on deposition temperature [15, 24].

Diamond seeding of the substrate, which is required for depositing high-quality diamond films, can be performed with a number of methods [25]. The most commonly applied methods include covering the substrate with diamond slurry and treating it ultrasonically [26, 27], coating substrates with carbon materials [28], using the interlayer containing nanodiamond [29, 30], and mechanical polishing of the substrate with diamond powder [31, 32]. Ma et al. observed the loss of transmittance due to the mechanical scratching of glass [16]. The processes of diamond deposition on quartz substrate and monocrystalline silicon have been compared by Daenen et al; the

authors used Ti interlayer for seeding and adhesion improvement [17]. In our work, we decided to omit the deposition of an additional adhesion interlayer, and thus potentially increase transmittance of the optical system.

To the best of our knowledge, the effect of high-power sonication seeding and the use of nanodiamond slurries on the structural and optical properties of chemical vapour deposited (CVD) diamond grown on fused silica optical fibres has not yet been reported. In this paper, we discuss the growth of microcrystalline (MCD) and NCD diamond thin films on fused silica optical fibres. Prior to diamond growth during CVD, the fibres had been seeded in a high-power sonication system by using two different suspensions of detonation nanodiamond (DND) and different time durations. In our study, we proposed to use the most common diamond suspensions reported by other groups as a standard ultrasonic diamond seeding media, i.e. diamond particles with the mean size of 5 nm suspended in dimethyl sulfoxide (DMSO-5 nm DND) [33–35], and the particles with the mean size of 50 nm suspended in deionised water (water-50 nm DND) [36, 37]. Diamond growth processes were performed using microwave plasma assisted chemical vapour deposition (MW PA CVD) system. The  $sp^3/sp^2$  band ratio, representing the quality of diamond layer, was measured using Raman spectroscopy. Morphology of the layers deposited on the fibres and seeding efficiency was investigated by using scanning electron microscopy (SEM). The growth rate of the films and their optical properties, i.e. refractive index and extinction coefficient were estimated using spectroscopic ellipsometry (SE).

## 2 Experimental details

### 2.1 Fibre seeding by the high-power sonication procedure

In our experiments, we used standard nanodiamond suspensions, i.e. diamond particles with the mean size of 5 nm suspended in dimethyl sulfoxide (DMSO-5 nm DND), and the particles with the mean size of 50 nm suspended in deionised water (water-50 nm DND). Tens of single-mode optical fibre (Corning SMF28) samples (approx. 3 cm in length) with a cladding diameter of 125  $\mu\text{m}$  were prepared, where both sample ends were cleaved and the polymer coatings were mechanically removed. The investigated optical fibre is made of fused silica cladding, which is high-quality amorphous  $\text{SiO}_2$ , and germanium-doped fused silica core (diameter of 8.2  $\mu\text{m}$ ). A set of p-type <100> silicon wafers were used as a reference sample. The fibres and silicon wafers were cleaned in the ultrasonic bath containing acetone for 5 min, then rinsed in 2-isopropanol and nitrogen dried.

Seeding was performed using a sonicator with the horn-type sonotrode. The samples of optical fibre and Si wafer were seeded during the same procedure in order to obtain similar surface preparation. Both optical fibres and Si wafers were placed at the bottom of glass vessel (approx. 7 cm in depth), which was afterwards filled up with the suspension (see Fig. 1) and immersed in cooling water. Then, the sonotrode tip was adjusted and dipped approximately 2 cm into the solution, keeping a 5 cm long distance between the sonotrode tip and the fibres. The distance between the samples and the sonotrode was optimized to disperse ultrasonic energy and at the same time keep the surface of fused silica and Si wafer away from the cavitation region, where erosion defects occur. However, some defects can be seen on the surface, which had most likely been induced by erosion cavities.

The glass vessel required cooling because the whole setup was heating up during the process; this was achieved by using a three-step heat exchange liquid-based system, i.e. solution, internal cooling water, and a water jacket.

For all seeded substrates, the sonication power was gradually increased to either 36 or 72 W. The sonication-aided seeding process took 45 min, which included 5 min for increasing the sonication power, 30 min for the main process, and 10 min for cooling the probe (without sonication). After stopping the process, the fibre samples were cleaned in isopropanol and dried in a stream of nitrogen.

## 2.2 Diamond growth on fibres

Diamond thin films were synthesized using MW PA CVD system (SEKI Technotron, Japan) on both optical fibre

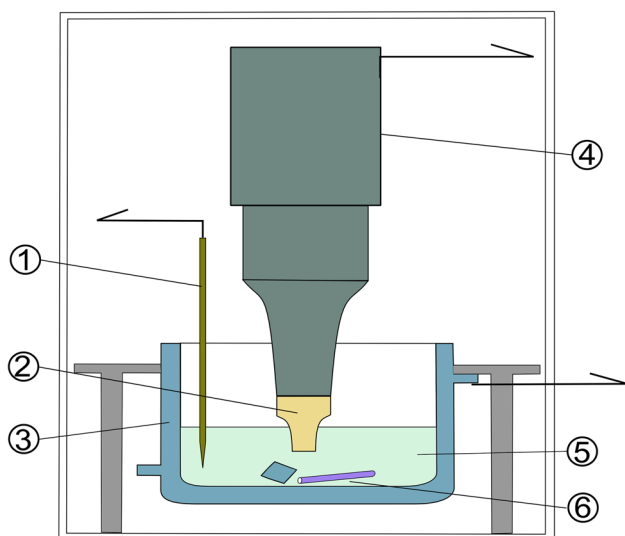


**Fig. 1** Schematic representation of seeding/cavitation system, where (1) is thermometer, (2) transducer, (3) glass vessel with a water jacket, (4) tip of the transducer, (5) suspension, and (6) fibres and Si wafer samples. The setup was installed in a sound-proof chamber

samples and the reference silicon wafers. Silica fibres were placed in stainless steel needles with a 1-cm lateral surface and the tip exposed to plasma. The reference Si wafers were placed inside CVD chamber on a molybdenum stage (see Fig. 2).

During the deposition process, the substrates were kept at 800 °C. Highly excited plasma was induced by microwave radiation (2.45 GHz). The plasma microwave power, which had been optimized for diamond synthesis, was maintained at 1,300 W [38–40]. The molar ratio of CH<sub>4</sub>–H<sub>2</sub> mixture was kept at 1 % of gas volume at 300 sccm of the total flow rate. The base pressure was about 10<sup>−6</sup> Torr, while the process pressure was kept at 50 Torr. The growth time was set to 30 and 180 min which resulted in the production of nano- and microcrystalline diamond films, respectively. The molecular composition of films was analysed by using Horiba LabRAM ARAMIS Raman spectroscope equipped with confocal microscope (100×/0.95 objective, 50 μm of confocal aperture) and 532-nm diode pumped solid state (DPSS). Raman spectra were recorded for both Si wafers and optical fibres and then fitted by means of OriginLab OriginPro v.8.0 and Thermo Scientific™ GRAMS AI to estimate sp<sup>3</sup>/sp<sup>2</sup> band ratio. Scanning electron microscope (S-3400N, HITACHI, Japan) with tungsten source and variable chamber pressure (VP-SEM) was used in order to assess the surface of films synthesized on the fibres and to estimate diamond seeding efficiency. No additional sample preparation was required before SEM analysis. To ensure an appropriate comparison of SEM images, all samples were assessed using the same microscope settings (secondary electrons mode with 20 kV accelerating voltage) and without pre-sputtering.

The diamond films grown on Si wafers were investigated with spectroscopic ellipsometry (SE). Optical investigations were carried out with a phase-modulated ellipsometer (UVISEL HORIBA Jobin–Yvon Inc., Edison, USA) for the wavelength range between 260 and 830 nm. The experiments were performed at room temperature

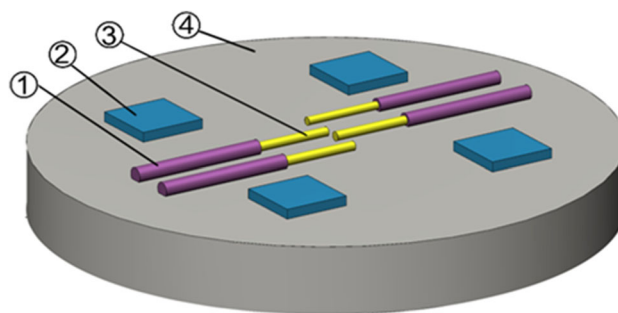


**Fig. 2** Schematic representation of the configuration of samples inside the plasma reactor during diamond growth, where (3) marks fibres in needles (1), and (2) indicates the reference samples on Mo stage (4)

using an angle of incidence of  $70^\circ$ . Ellipsometric fitting was based on a four-phase optical model (air/roughness/diamond/Si wafer). The roughness phase on the diamond surface was modelled as an effective mixture of a diamond film and space filled with air [23]. Such approach allowed for estimating the average surface roughness of the samples. The dispersion of Si <100> was taken from the database [41]. The diamond film has been assumed to be an isotropic, homogeneous material and its dispersion was fitted to the Tauc–Lorentz oscillator (TL) model. Such approach has been recently applied by Zimmer et al. [42] for boron-doped NCD films, Hu et al. [15] for MCD films, and Jellison et al. [43] for amorphous semiconductors. The model is a combination of the Tauc joint density of states [44] and the quantum mechanical Lorentz oscillator model [45]. The TL model fits to the dielectric functions of a class of amorphous materials. Such materials exhibit a peculiarity due to the presence of two separated contributions of inter-band electronic transition related to  $sp^2$  and  $sp^3$  bonded carbon [46]. The parameters of the TL model were fitted for each of the analysed films. Finally, the assumed optical model was fitted to the experimental data using the nonlinear Levenberg–Marquardt regression method for mean-square error (MSE) minimization [47]. As a result of SE analysis, the thickness and optical constants, i.e. refractive index  $n(\lambda)$  and extinction coefficient  $k(\lambda)$ , were obtained.

### 3 Results

#### 3.1 The influence of seeding procedure on the morphology and structure of diamond films deposited on fibres

The effect of high-power sonication seeding process on the morphology of diamond films deposited on optical fibres was investigated for different sonication power, time of deposition, and the composition of sonication suspension. In Fig. 3, the morphology of the resulting diamond films on fibres, sonicated in the suspension of 5-nm nanodiamond particles in DMSO, is presented. After a 30-min deposition, close to complete surface coverage with the diamond layer was observed. The average size of crystals was dependent on deposition time, i.e. after 30 min of deposition the grain size reached 200 nm, while after 180 min grains exceeding 1,000 nm in size could be found. Moreover, it was observed that the layer homogeneity and the crystal size greatly increased with increasing sonication power for longer deposition times.

For comparative purposes, the SEM images of diamond films obtained after sonication in the water-based suspension are presented in Fig. 4. It is noteworthy that in the case

of DI water-based suspension, a 30-min deposition did not result in the complete surface coverage of samples seeded via sonication at either 36 or 72 W. However, a longer deposition led to both an increase in coverage and the growth of crystals. The same effect was observed while using the DMSO-based suspension. It must be emphasized here that in the case of water-based suspension used during the sonication process, after 180 min of deposition with a sonication power of 72 W the mean grain size still remained smaller compared with the similar process with the application of DMSO-based suspension. For the lower sonication power, the influence of the solution type on the growth rate was negligible.

The seeding efficiency expressed here as seeding density was estimated by counting the total number of diamond grains in defined surface the area ( $120 \mu\text{m}^2$ ). The results of this basic calculation are shown in Table 1. The calculations assuming that seeding of glass fibres in water-based suspension (water-50 nm DND) gives maximum nucleation densities of  $4.5 \times 10^9$  (36 W) and  $5 \times 10^9 \text{ cm}^{-2}$  (72 W), while DMSO-based suspension (DMSO-5 nm DND) value of approximately  $3.5 \times 10^9 \text{ cm}^{-2}$ . Achieved here seeding density level is smaller than values ( $1 \times 10^{11} \text{ cm}^{-2}$ ) reported by other groups [48, 49]. However, Yang et al. [48] and Butler et al. [49] results were achieved on Si wafers or glass plates but not on optical fibres, which are fragile and not resistant to bending or mechanical processing. This trend suggests that not only the size of DND nanoparticles in suspension influence on seeding density. It could be explained by protolysis of silanol groups that undergo on the fused silica surface in the aqueous solution [37]. Moreover, it was reported that the zeta potential of the fused silica substrate was negative in the aqueous solution [50] enabling to achieve higher seeding density [51].

The crystal sizes and their distribution for the obtained films were estimated from the measurements made on  $120 \mu\text{m}^2$  of the sample area at  $0.5 \mu\text{m}$  intervals (see Table 1). The relative amount of counts was calculated taking into consideration the number of crystals of certain diameter in the given area.

For both sonication procedures, (111) facets of diamond crystals dominated. Moreover, an increase in sonication power resulted in decreased number of (100) facets. The suspension type (DMSO vs. water) seemed to have no effect on facets. Finally, the SEM micrographs of the films obtained on optical fibres (see Fig. 5) allowed for formulating a general conclusion that the high-power sonication seeding and the application of DMSO as a dispersant resulted in better homogeneity of the film structure and film continuity compared with the treatment with low power and sonication in water medium.

The surface of optical fibre after the cavitation treatment is shown in Fig. 6a. As a result of the occurrence of high-



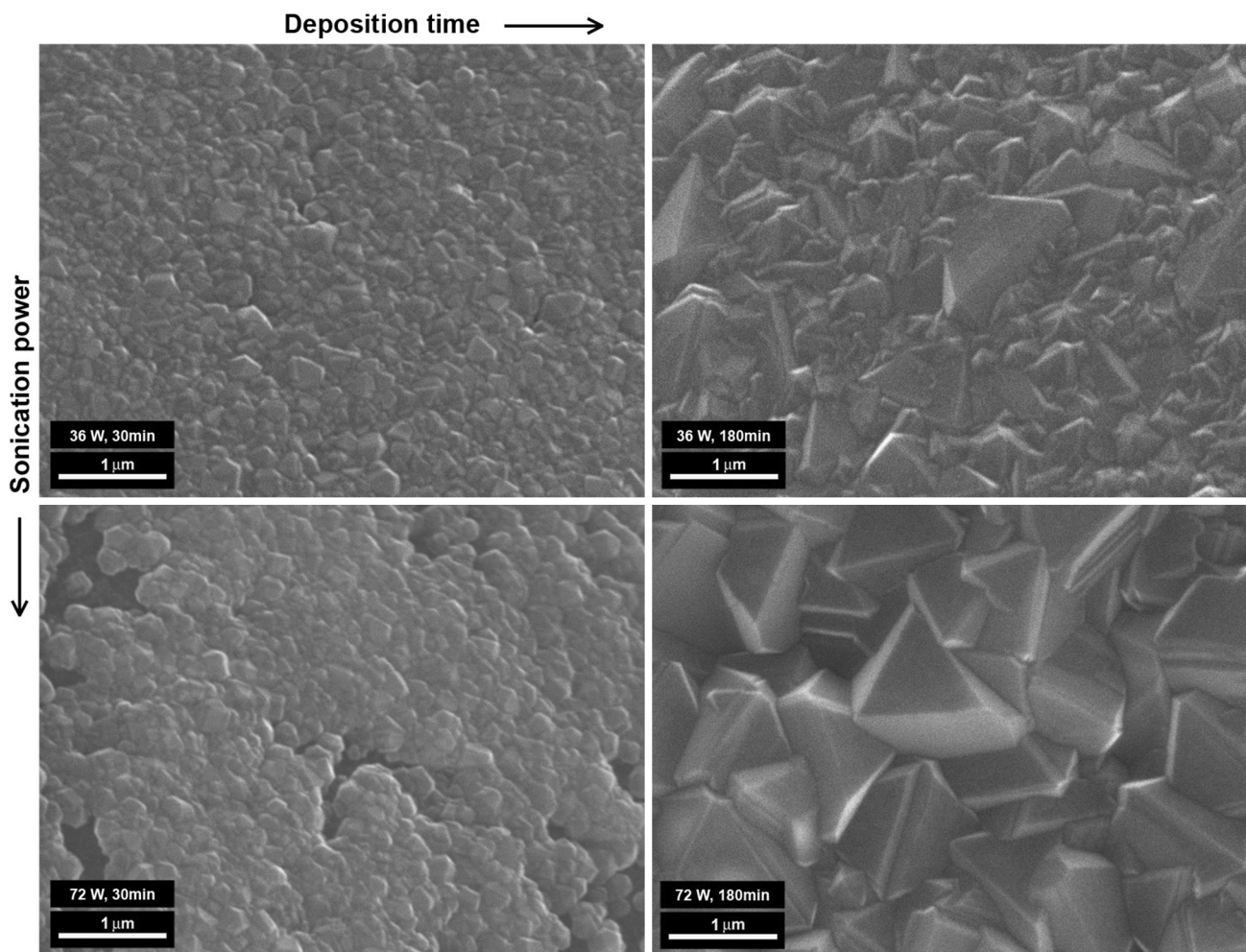


**Fig. 3** SEM images ( $\times 20,000$  magnification) showing the morphology of diamond films deposited on optical fibres for different sonication power and deposition times. The seeding was performed in DMSO-based suspension

energy sound during the procedure, the fibre erosion had taken place. The mean surface roughness increased significantly due to this interaction. Moreover, additional shallow cavities of 5–20 μm in diameter are visible. The cavities are randomly distributed on the surface. The optical fibre that had been subjected to the cavitation pretreatment was afterwards coated with diamond. In Fig. 6b, many holes can be seen on the surface of coating, which had most likely been induced by erosion cavities. The dimensions of the holes are similar. Apart from the holes, the fibre surface is uniformly covered with the film. No cracks or heterogeneities can be observed.

Raman spectra of the films deposited on fibres are shown in Fig. 7, while the calculated parameters of these films are given in Table 2.

In all spectra, a sharp and strong Raman band assigned to  $sp^3$  diamond lattice can be seen at about  $1,332\text{ cm}^{-1}$ , which confirms that polycrystalline diamond films were deposited. Moreover, wide bands at about  $1,540\text{ cm}^{-1}$ ,

assigned to amorphous  $sp^2$  phase, are visible. The band at  $1,332\text{ cm}^{-1}$  was fitted by a Lorentz profile, while the band at  $1,540\text{ cm}^{-1}$ , by a Gaussian profile. The  $sp^3/sp^2$  band ratio was expressed as the ratio of the areas under those bands. Such a ratio allows for comparing the quality and crystallinity of different layers, i.e. higher  $sp^3/sp^2$  band ratio refers to larger size of diamond crystals as well as lower amount of unwanted amorphous phase.

Comparison of sonication with use of water and DMSO made by Raman spectroscopy shows that in case of deposition on fused silica efficiency of both materials was rather similar for growth time of 180 min, while for short growth time DMSO was slightly better. Especially, diamond lines were significantly narrower, which suggests that better crystallinity was obtained. Thus, it can be concluded that DMSO-based process is more suitable for deposition of very thin layers.

More influential were growth time and power of sonication. Based on the analysis of Raman spectra (see

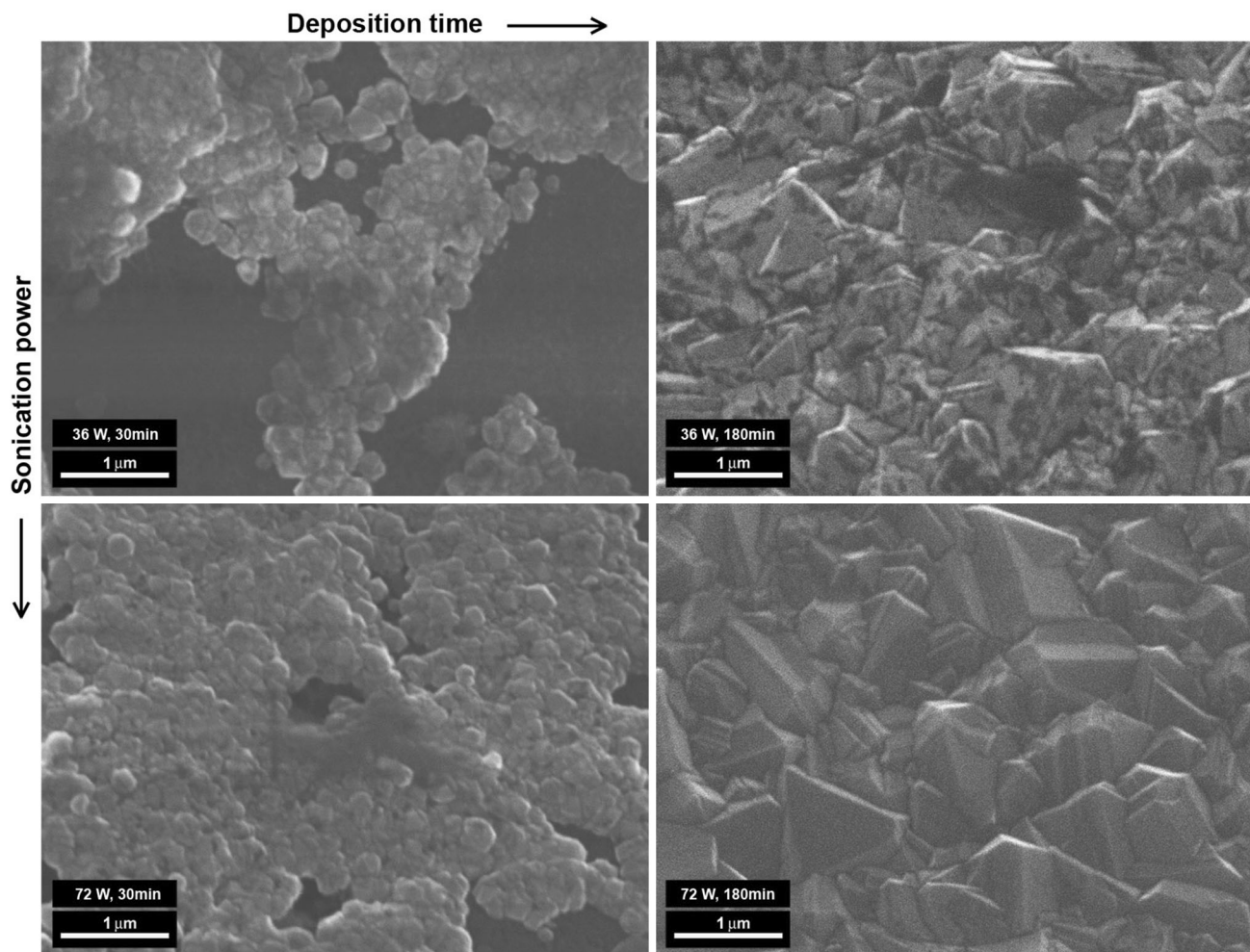


**Fig. 4** SEM images ( $\times 20,000$  magnification) showing the morphology of diamond films deposited on optical fibres for different sonication power and deposition times. The seeding was performed in DI water-based suspension

**Table 1** Seeding nucleation density and crystal size distribution on the surface of diamond film for different sonication conditions after 180 min of deposition

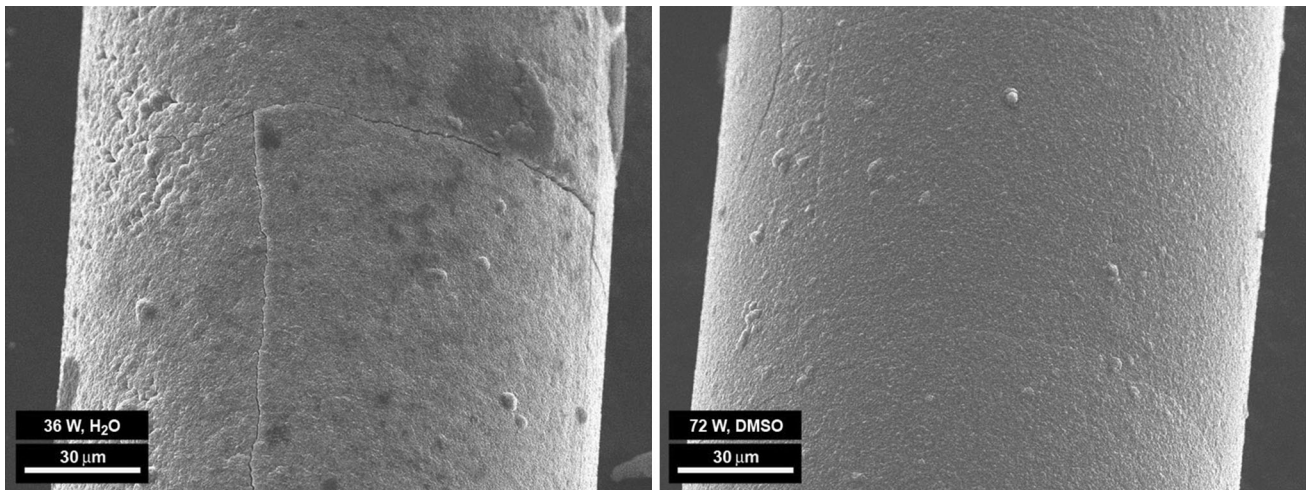
Seeding mode	36 W (water-50 nm DND)	72 W (water-50 nm DND)	36 W (DMSO-5 nm)	72 W (DMSO-5 nm DND)
Seeding density ( $\text{cm}^{-2}$ )	$4.5 \times 10^9$	$5 \times 10^9$	$3.5 \times 10^9$	$3.5 \times 10^9$
Surface grain size ( $\mu\text{m}$ )				
<0.5	54 %	59 %	83 %	7 %
0.5–1	37 %	26 %	10 %	34 %
1–1.5	8 %	15 %	7 %	45 %
1.5>	1 %	0 %	0 %	14 %

Table 2), it can be concluded that for all sets of sonication parameters, quality of the layers, determined by  $\text{sp}^3/\text{sp}^2$  band ratio and Raman line width, was better for growth

time equal to 180 min than for growth of 30 min. It is in good agreement with expectations and it can be explained by more intensive growth of  $\text{sp}^2$  phase close to the amorphous substrate surface. Moreover, it can be noticed that the sonication power of 72 W results in better crystallinity of the deposited layers than a power of 36 W—the width of the band assigned to  $\text{sp}^3$  phase is lower—which means that the diamond lattice is less distorted. Moreover, in most cases,  $\text{sp}^3/\text{sp}^2$  band ratio is better for 72 W.

Slightly different results were obtained for process carried out 180 min when DMSO and 36 W of sonication power. Unexpected width and shift of the “diamond” band to  $1,325.8 \text{ cm}^{-1}$  in the case of this sample can be explained by the more intensive lattice stress and consequent  $\text{sp}^3$  distortion. This finding confirms that the deposited layers are under stress because of the different crystal structures of film and the fused silica substrate. Therefore, the deposition process requires further optimization in order to avoid cracking of the film, and to enable deposition of films





**Fig. 5** SEM images ( $\times 700$  magnification) of diamond films on optical fibres obtained in different suspension types (water vs. DMSO) and at different levels of sonication power

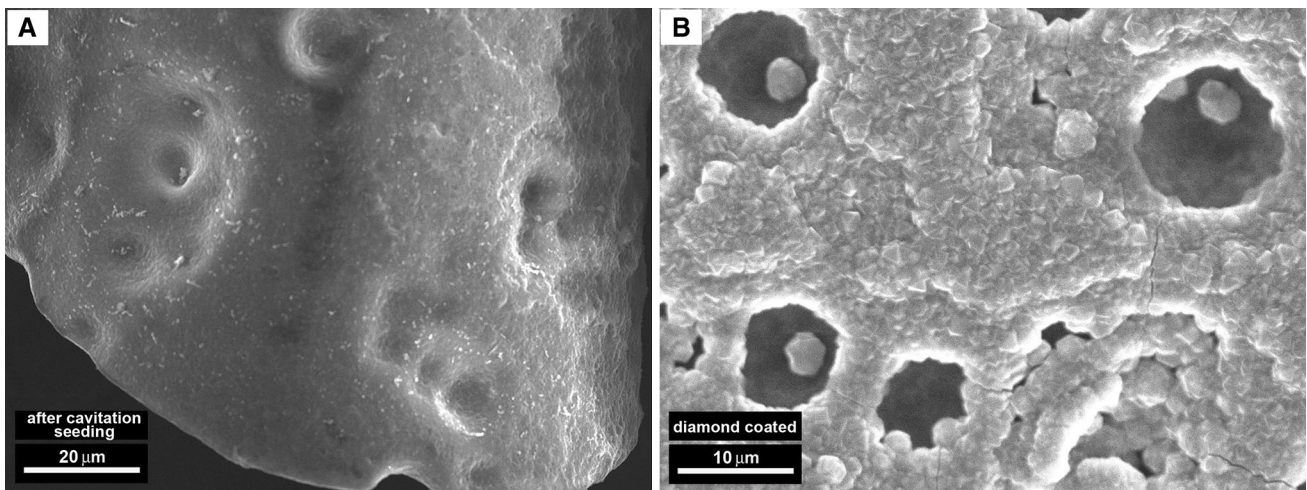


**Fig. 6** Erosion/cavitation defects on the fibre surface which occurred during high-power ultrasonic seeding; **a** depicts the surface after seeding, and **b** surface after the diamond deposition

with larger surface areas. A decrease in the Raman band width for a longer deposition time (with only one exception, i.e. DMSO and 72 W of sonication power), which should correspond to less distorted  $sp^3$  phase, is in good agreement with an increase in the mean grain size observed by SEM.

### 3.2 The influence of seeding procedure on the optical properties of diamond films

Due to difficulty of making ellipsometric measurements directly on the curved surface of optical fibres, the determinations were made instead on the reference samples with diamond films deposited on Si wafers. The applied fitting procedure gives accurate values of the film thickness and roughness, and its optical properties. The ellipsometric

analysis was performed on fully encapsulated diamond films only. The list of films analysed by SE, including their properties, is presented in Table 3. The film thickness mainly depends on deposition time. However, slight differences in the growth rate, induced by other deposition parameters, were also observed. It was found that the growth rate increases for the higher level of sonication power. At 72 W, the seeding density was higher (see SEM results in Figs. 3, 4) resulting in an increase in the film growth. For samples subjected to long deposition (i.e. 180 min), the film surface displayed higher roughness and a microcrystalline character. For a 30-min deposition, the film surface had lower roughness, a feature typical for nanocrystalline structure. The application of DMSO resulted in the highest roughness which was still acceptable in relation to the possible use of the produced optical fibres

**Fig. 7** Raman spectra of films deposited on fibres; **a** 30-min deposition time, **b** 180-min deposition time

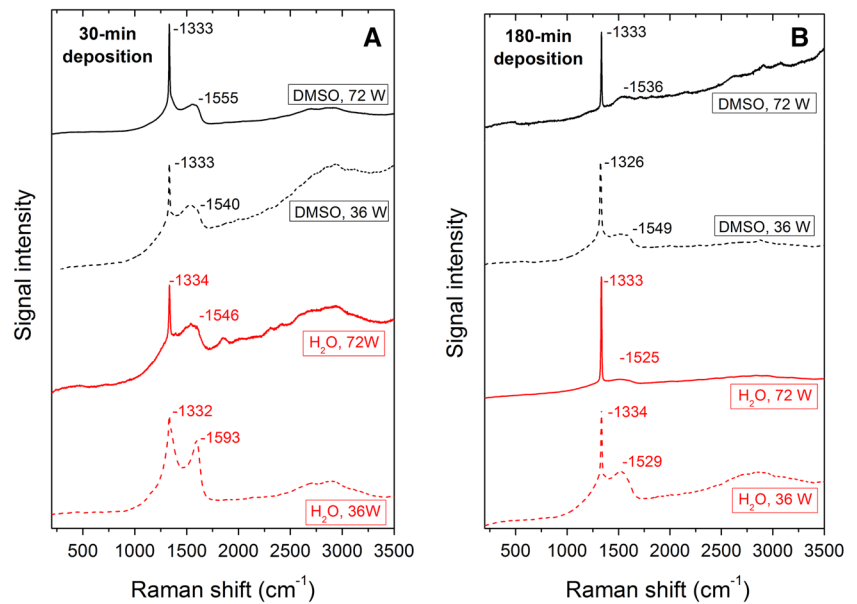


**Table 2** Intensity ratio of Raman bands assigned to  $sp^3$  and  $sp^2$  phase ( $sp^3/sp^2$ ) as well as the position ( $D_{PP}$ ) and width ( $D_{FWHM}$ ) of Raman “diamond” band in the deposited films

DND suspension	Growth time (min)	72 (W)		Power of sonication			
		$sp^3/sp^2$	$D_{PP}$	$D_{FWHM}$	$sp^3/sp^2$	$D_{PP}$	$D_{FWHM}$
Water (50 nm DND)	30	0.22	1,334.0	13.4	0.07	1,332.5	16.0
	180	0.61	1,332.7	8.9	0.29	1,333.6	12.0
DMSO (5 nm DND)	30	0.25	1,332.6	9.2	0.15	1,332.5	11.5
	180	0.44	1,333.5	8.1	0.59	1,325.8	16.0

**Table 3** The parameters of diamond films deposited on the reference Si wafers, as determined by SE

Sonication power (W)	Seeding solution	Deposition time (min)	Film thickness (nm)	Growth rate ( $nm\ min^{-1}$ )	Surface roughness (nm)	Optical density (a.u.)
36	Water (50 nm DND)	180	480	2.7	20	0.94
	DMSO (5 nm DND)	180	450	2.5	26	0.96
		30	90	3	10	0.83
72	Water (50 nm DND)	180	600	3.3	24	0.98
	DMSO (5 nm DND)	180	530	2.9	32	0.98
		30	110	3.7	12	0.86

in sensors [52]. High roughness was in agreement with the grain size distribution estimated from SEM analysis (Fig. 3; Table 1). The increased roughness can be explained by lower seeding density occurring for lateral expansion of the grains. The DMSO-based seeding suspension had lower polarity index than the water-based one. High polarity index effectively increases seeding. However, the DI water-based suspensions are unstable compared to those based on DMSO [26]. When the roughness effect is neglected, the optical density ( $\rho_{opt}$ ) of the deposited diamond films can be estimated using Eq. (1), where  $n_d$  and  $n$  are the refractive indices of single-crystal diamond (SCD) and polycrystalline diamond films, respectively [15].

$$\rho_{opt} = \frac{n^2 - 1}{n^2 + 2} \cdot \frac{n_d^2 + 2}{n_d^2 - 1} \quad (1)$$

The obtained optical density, relative to SCD, reached the values of 0.83 for NCD films (30-min deposition) and 0.98 for MCD films (180 min). The high optical density can be attributed to the high content of  $sp^3$  hybridization phase, which was confirmed by Raman spectroscopy (see Fig. 7). Our recently published results [53] and those reported by Hu et al. [15] show a ca. 10 % decrease of optical density in the films obtained on silica glass substrates in comparison with the films produced on Si wafers.



Besides the structural properties of films and their morphology, SE was used to determine the optical properties of the obtained films. In Fig. 8, the dispersion characteristics of the layers  $n$  and  $k$  for the diamond films deposited by using different DND seeding suspensions are presented. The  $n$  value for SCD was added in Fig. 8 as a Ref. [41]. The optical properties decreased with increasing wavelength, and at the same time, the films displayed normal dispersion and a behaviour typical for the band gap of electronic transition. Surprisingly, the seeding suspension type had no significant effect on the values of  $n$  and  $k$  in the films grown for 180 min. The obtained  $n$  values (2.52–2.37) were smaller than those for SCD. In comparison, Hu et al. [15] reported the variability of  $n$  between 2.31 and 2.34 for NCD films, while Gupta et al. [54] determined the  $n$  values between 1.7 and 2.1 for MCD films at  $\lambda = 632$  nm. The lower  $n$  values (compared to SCD) indicated lower physical density of the films [55, 56]. The  $k$  values obtained in this study were close to zero for

wavelengths above 380 nm for both seeding suspension types. At 230 nm, the  $k$  values reached the maxima of 0.8 and 0.6 for water- and DMSO-based suspensions, respectively.

The values of  $n$  and  $k$  of diamond films grown on Si wafers, which had been pre-treated by seeding at different sonication power and deposition times, are shown in Fig. 9ab. It is noticeable that  $n$  increases with increasing sonication power and deposition time. The use of lower sonication power resulted in the reduced amount of erosion defects, but it also decreased the  $n$  value by approximately 0.05. The effect of lowered  $n$  can be explained by lower seeding efficiency and higher amount of  $sp^2$  hybridization phase in between crystalline grains causing the reduction of  $sp^3/sp^2$  band ratio, as confirmed by Raman spectroscopy. Also, a shorter deposition time (30 min) resulted in lowered  $n$  value (2.05–2.25), typical nanocrystalline “cauliflower-like” morphology (see Fig. 4), and a relatively high  $sp^2$  content observed via Raman spectroscopy (see Fig. 7).

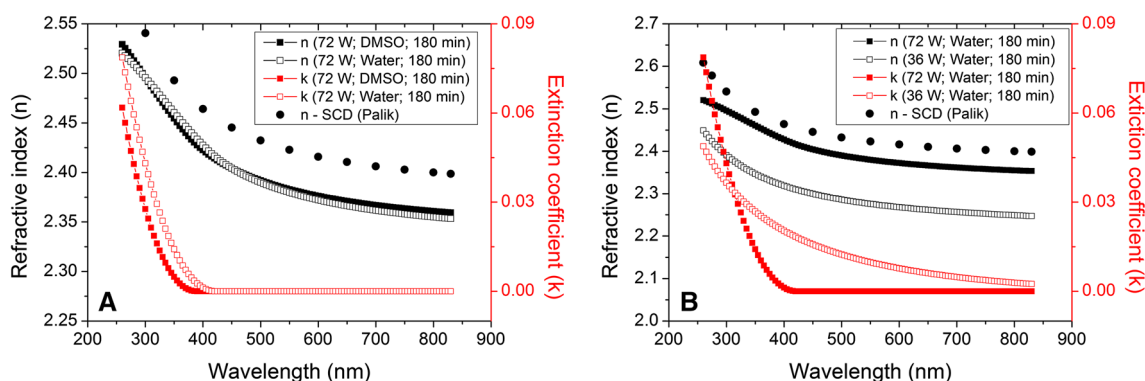


**Fig. 8** Dispersion of refractive index and the extinction coefficient of diamond films seeded in different suspension types. The sonication power was 72 W, and deposition time was 180 min. The  $n$  value for (circle)-SCD was plotted for comparative purposes [41]

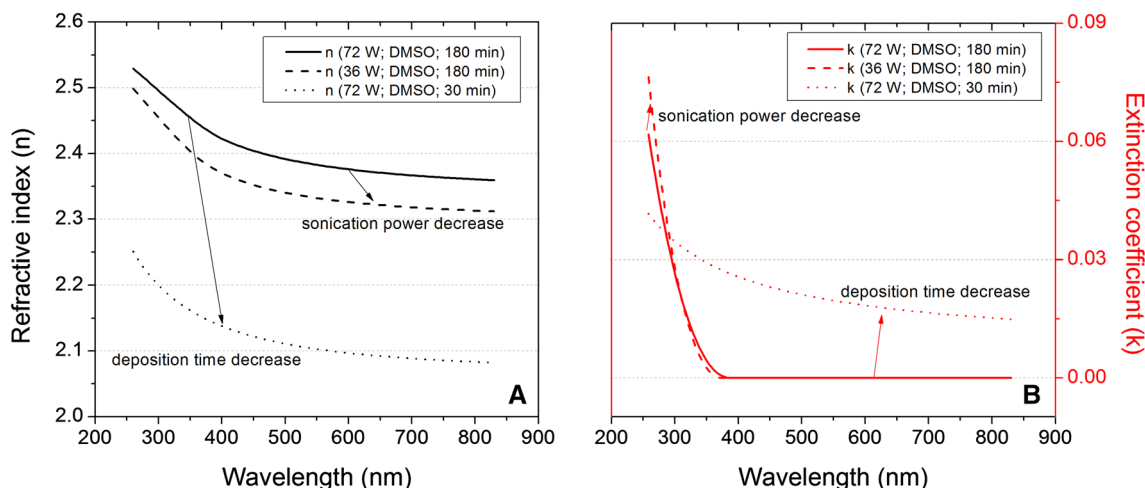


**Fig. 9** Dispersion of refractive index **a** and the extinction coefficient, **b** of diamond films seeded in DMSO-5 nm DND suspension at different deposition times (30 and 180 min) and sonication power (36 and 72 W). Trends are marked by arrows

The application of short deposition time during the experiment was aimed at limiting the thickness of diamond film. For the films produced under such conditions, besides the low thickness, we also observed a significant decrease in the film's internal stress and surface roughness. SE studies demonstrated that the short deposition time results in samples displaying optical properties which fulfil the requirements for their application in fused silica optical fibre sensors; the  $n$  value of 2.05 gives high refractive index contrast compared with 1.47 for fused silica (see Fig. 9a). Moreover, it is noteworthy that the  $k$  value in such films reached 0.15; therefore, they can limit light propagation by high optical absorption. The absorption coefficient of the films, defined as  $\alpha$  ( $=2\pi k$ ), reached the value of 1.2. In comparison,  $\alpha$  for MCD films deposited during the 180-min process was close to zero. Nevertheless, considering the optical sensing applications, the estimated NCD absorption coefficient is not critical because the penetration depth  $D_\lambda$  ( $=\lambda \cdot \alpha^{-1}$ ) [47] at  $\lambda = 632$  nm reached 526 nm, while the 30-min deposition resulted in the film thickness of approximately 100 nm. The  $k$  values obtained at  $\lambda = 632$  nm are comparable to those reported by Hu et al. (0.015 for NCD films) [15] and Gupta et al. (0.07–0.315) [54]. The samples grown during a short deposition process (30 min) on the substrates seeded in water-based suspension were not investigated by SE due to the incomplete surface encapsulation of films (see Fig. 3). The increase in sonication power from 36 to 72 W had a negligible influence on the  $k$  value (see Fig. 9b); therefore, it has been concluded that the power of 36 W can be effectively used for diamond seeding. However, it should be underlined that the lower sonication power limits the size and amount of the substrates in one seeding process. The limitation originates from the lower volume of suspension which could be effectively ultrasonically supplied when the power is decreased.

#### 4 Conclusion

Polycrystalline CVD diamond films were grown on fused silica fibres using MW PA CVD and high-power sonication seeding procedure. The influence of standard detonation nanodiamond suspensions, i.e. DND dispersed in (1) DMSO, and (2) deionised water was investigated. SEM analysis demonstrated that the application of DMSO-based suspension enhances the substrate encapsulation during the 30-min deposition process, with the growth rate reaching approximately  $4 \text{ nm min}^{-1}$ . The 180-min deposition resulted in the formation of microcrystalline layer, while the 30-min process favoured the NCD structure.

Raman spectra showed that the highest  $\text{sp}^3/\text{sp}^2$  band ratio was obtained for the sonication performed in water-

based suspension at 72 W, and longer deposition time. For shorter deposition times, the DMSO-based suspension should be used during sonication. The sonication power of 72 W and a deposition time of 180 min allow for achieving high refractive index (2.38 at  $\lambda = 632$  nm) and low extinction coefficient of the deposited film. The values of  $n$  increased proportionally to the sonication power, while they showed a significant increase with increasing deposition time. Nevertheless, the lower sonication power allowed for reducing the amount of erosion defects on the fibre surface. The lower sonication power induced higher  $\text{sp}^3$  content in the film. Moreover, different seeding suspensions did not significantly affect the  $n$  and  $k$  values of the diamond films deposited during a 180-min process. However, the 30-min-long growth preceded by seeding in DMSO-based suspension, allowed for obtaining shorter nucleation and faster substrate encapsulation compared with the structures resulting from seeding in water-based suspension. In comparison with water-based suspension, the seeding in DMSO resulted in the higher values of mean surface roughness ( $\sim 32$  nm). This finding can be explained by lower seeding density which induces the lateral-grain expansion. In conclusion, the high-power sonication procedure is a very efficient and flexible technique for seeding of fused silica optical fibres.

**Acknowledgments** This work was supported by the Polish National Science Center (NCN) under grant No. 2011/03/D/ST7/03541 and by the National Centre for Research and Development (NCBiR) under Project No. LIDER/20/91/L-2/10 and LIDER/03/16/L-2/10. The DS funds of the Faculty of Electronics, Telecommunications and Informatics at the Gdansk University of Technology are also acknowledged.

**Open Access** This article is distributed under the terms of the Creative Commons Attribution License which permits any use, distribution, and reproduction in any medium, provided the original author(s) and the source are credited.

#### References

1. B. Lee, Opt. Fiber Technol. **9**, 57 (2003)
2. S. Nesson, A.H. Hsieh, M. Yu, X. Zhang, J. Biomed. Opt. **13**, 044040 (2008)
3. S. Vurpillot, D. Inaudi, J.-M. Ducret, Proc. SPIE **2719**, 141 (1996)
4. M. Jedrzejewska-Szczerska, R. Bogdanowicz, M. Gnyba, R. Hyspser, B.B. Kosmowski, Eur. Phys. J. Spec. Top. **154**, 107 (2008)
5. P.M. Herbert, T.A. Gauthier, C.L. Briens, M.A. Bergougnou, Powder Technol. **80**, 243 (1994)
6. J.M. Fini, Meas. Sci. Technol. **15**, 1120 (2004)
7. H.-C. Lin, S.-T. Shiue, Y.-H. Cheng, T.-J. Yang, T.-C. Wu, H.-Y. Lin, Carbon **45**, 2004 (2007)
8. S.-T. Shiue, J.-L. He, L.-Y. Pan, S.-T. Huang, Thin Solid Films **406**, 210 (2002)
9. J. Stotter, J. Zak, Z. Behler, Y. Show, G.M. Swain, Anal. Chem. **74**, 5924 (2002)

10. M. Smietana, J. Szmids, M.L. Korwin-Pawłowski, W.J. Bock, J. Grabarczyk, *Diam. Relat. Mater.* **16**, 1374 (2007)
11. M. Smietana, M.L. Korwin-Pawłowski, W.J. Bock, G.R. Pickrell, J. Szmids, *Meas. Sci. Technol.* **19**, 085301 (2008)
12. P.W. May, C.A. Rego, M.N.R. Ashfold, K.N. Rosser, G. Lu, T.D. Walsh, L. Holt, N.M. Everitt, P.G. Partridge, *Diam. Relat. Mater.* **4**, 794 (1995)
13. N.J. Alberto, J.A. Santos, C.A.F. Marques, V.F.S. Neto, R.N. Nogueira, in *OFS2012 22nd International Conference on Optical Fiber Sensors*, ed. by Y. Liao, W. Jin, D.D. Sampson, R. Yamauchi, Y. Chung, K. Nakamura, Y. Rao. Proceedings of SPIE, vol. 8421 (SPIE, Bellingham, 2012)
14. M. Smietana, J. Szmids, M. Dudek, P. Niedzielski, *Diam. Relat. Mater.* **13**, 954 (2004)
15. Z.G. Hu, P. Prunici, P. Hess, K.H. Chen, *J. Mater. Sci. Mater. Electron.* **18**, 37 (2007)
16. Z.B. Ma, J.H. Wang, W.W. Zhang, A.H. He, *Surf. Coat. Technol.* **184**, 307 (2004)
17. M. Daenen, O.A. Williams, J. D'Haen, K. Haenen, M. Nešládek, *Phys. Stat. Solidi* **203**, 3005 (2006)
18. T. Lohner, P. Csikvári, P. Petrik, G. Hárs, *Appl. Surf. Sci.* **281**, 113 (2013)
19. S. Gupta, B.R. Weiner, G. Morell, *J. Appl. Phys.* **90**, 1280 (2001)
20. V. Prajzler, M. Varga, P. Nekvindova, Z. Remes, A. Kromka, *Opt. Express* **21**, 8417 (2013)
21. T. Sharda, T. Soga, T. Jimbo, *J. Appl. Phys.* **93**, 101 (2002)
22. S. Gupta, B.R. Weiner, G. Morell, *J. Appl. Phys.* **92**, 5457 (2002)
23. S. Gupta, B.R. Weiner, G. Morell, *Diam. Relat. Mater.* **10**, 1968 (2001)
24. Z.G. Hu, P. Hess, *Appl. Phys. Lett.* **89**, 081906 (2006)
25. J. Asmussen, D.K. Reinhard, *Diamond Films Handbook* (CRC Press, Boca Raton, 2002)
26. O. Shenderova, S. Hens, G. McGuire, *Diam. Relat. Mater.* **19**, 260 (2010)
27. O.A. Williams, O. Douhéret, M. Daenen, K. Haenen, E. Ōsawa, M. Takahashi, *Chem. Phys. Lett.* **445**, 255 (2007)
28. A. Kromka, O. Babchenko, H. Kozak, K. Hruska, B. Rezek, M. Ledinsky, J. Potmesil, M. Michalka, M. Vanecek, *Diam. Relat. Mater.* **18**, 734 (2009)
29. M. Tsigkourakos, T. Hantschel, S.D. Janssens, K. Haenen, W. Vandervorst, *Phys. Stat. Solidi* **209**, 1659 (2012)
30. E.I. Givargizov, V.V. Zhiraov, A.V. Kuznetsov, P.S. Plekhanov, *Mater. Lett.* **18**, 61 (1993)
31. Y. Lifshitz, C.H. Lee, Y. Wu, W.J. Zhang, I. Bello, S.T. Lee, *Appl. Phys. Lett.* **88**, 243114 (2006)
32. D.M. Gruen, *Annu. Rev. Mater. Sci.* **29**, 211 (1999)
33. X. Liu, T. Yu, Q. Wei, Z. Yu, X. Xu, *Colloids Surf. Physicochem. Eng. Asp.* **412**, 82 (2012)
34. M. Tsigkourakos, T. Hantschel, S.D. Janssens, K. Haenen, W. Vandervorst, *Phys. Stat. Solidi* **209**, 1659 (2012)
35. O. Shenderova, S. Hens, G. McGuire, *Diam. Relat. Mater.* **19**, 260 (2010)
36. O.A. Williams, O. Douhéret, M. Daenen, K. Haenen, E. Ōsawa, M. Takahashi, *Chem. Phys. Lett.* **445**, 255 (2007)
37. H.-J. Lee, H. Jeon, W.-S. Lee, *J. Phys. Chem. C* **116**, 9180 (2012)
38. R. Bogdanowicz, *Acta Phys. Pol.* **114**, A33 (2008)
39. R. Bogdanowicz, M. Gnyba, P. Wroczyński, *J. Phys. IV Proc.* **137**, 57 (2006)
40. R. Bogdanowicz, M. Gnyba, P. Wroczyński, B.B. Kosmowski, *J. Optoelectron. Adv. Mater.* **12**, 1660 (2010)
41. E.D. Palik, *Handbook of Optical Constants of Solids* (Academic Press, New York, 1998)
42. A. Zimmer, O.A. Williams, K. Haenen, H. Terryn, *Appl. Phys. Lett.* **93**, 131910 (2008)
43. G.E. Jellison Jr, V.I. Merkulov, A.A. Poretzky, D.B. Geohegan, G. Eres, D.H. Lowndes, J.B. Caughman, *Thin Solid Films* **377–378**, 68 (2000)
44. M. Gioti, D. Papadimitriou, S. Logothetidis, *Diam. Relat. Mater.* **9**, 741 (2000)
45. M. Gioti, S. Logothetidis, *Diam. Relat. Mater.* **12**, 957 (2003)
46. G.E. Jellison Jr, F.A. Modine, *Appl. Phys. Lett.* **69**, 371 (1996)
47. H. Tompkins, E.A. Irene, *Handbook of Ellipsometry* (William Andrew, Norwich, 2005)
48. W.B. Yang, F.X. Lü, Z.X. Cao, *J. Appl. Phys.* **91**, 10068 (2002)
49. J.E. Butler, A.V. Sumant, *Chem. Vap. Depos.* **14**, 145 (2008)
50. C. Schwer, E. Kenndler, *Anal. Chem.* **63**, 1801 (1991)
51. J. Hees, A. Kriele, O.A. Williams, *Chem. Phys. Lett.* **509**, 12 (2011)
52. F.J. Arregui, *Sensors Based on Nanostructured Materials* (Springer, Boston, 2009)
53. R. Bogdanowicz, M. Śmietana, M. Gnyba, M. Ficek, V. Straňák, Ł. Goluński, M. Sobaszek, J. Ryl, *Phys. Stat. Solidi* **210**, 1991 (2013)
54. S. Gupta, B.R. Weiner, G. Morell, *J. Appl. Phys.* **90**, 1280 (2001)
55. J. Robertson, *Mater. Sci. Eng. R Rep.* **37**, 129 (2002)
56. G. Davies, *Properties and Growth of Diamond* (INSPEC, The Institution of Electrical Engineers, 1994)